CHEMISTRY OF MATERIALS

VOLUME 14, NUMBER 12 DECEMBER 2002

Articles

Palladium-Containing Zeolite Beta Macrostructures Prepared by Resin Macrotemplating

Valeri Naydenov, Lubomira Tosheva,* and Johan Sterte

Division of Chemical Technology, Luleå University of Technology, S-971 87 Luleå, Sweden

Received February 26, 2002. Revised Manuscript Received August 28, 2002

A multistep procedure for the preparation of palladium-containing zeolite beta spheres using anion-exchange resin beads as shape-directing macrotemplates is presented. In a first step, resin beads are hydrothermally treated with zeolite beta synthesis solutions, and as a result resin−zeolite beta composite particles are obtained. In a second step, anionic palladium precursor species are introduced into the composite using the residual ion-exchange capacity of the resin. Finally, the ion exchanger is removed by calcination, leaving self-bonded palladium-containing zeolite beta spheres. The spheres obtained by the procedure were characterized by AAS, XRD, SEM, EDS, UV−vis DRS spectroscopy, nitrogen adsorption measurements, and chemisorption. Materials with controlled macroshape, porosity, and palladium content were prepared by the method.

Introduction

Employing zeolites as hosting materials has become a common feature in the preparation of multicomponent heterogeneous catalysts. The active sites in such catalytic systems are usually generated by the introduction of transition metal ions into either extraframework or framework positions. The advantages that make zeolites more attractive than amorphous inorganic oxides as supports are the following: (i) high surface area mainly hidden within the unique and strictly defined intrazeolite architectures; (ii) finely adjustable concentrations of Brønsted acidic centers achieved by controlling the Si/Al ratio during or after the zeolite synthesis; and (iii) thermal stability. Noble metal crystallites supported on zeolites result in a bifunctional catalyst with a dehydrogenation−hydrogenation activity due to the metal sites, whereas the zeolite acidic centers are responsible for alkylcarbenium ion rearrangements.[1−12] Zeolite-supported palladium materials have also been reported to be active catalysts for the selective catalytic reduction

* To whom correspondence should be addressed. Phone: +46-920-492-934. Fax: +46-920-491-199. E-mail: luto@km.luth.se.

(1) van Bekkum, H.; Flanigen, E. M.; Jacobs, P. A.; Jansen, J. C. *Stud. Surf. Sci. Catal.* **2001**, *137*, 892.
(2) Chica, A.; Corma, A. *J. Catal.* **1999**, *187*, 167.
(3) Gallezot, P. *Catal. Rev. Sci. Eng.* **1979**, *20*, 121.
(4) Raybaud, P.; Patrigeon, A.; Toulhoat, H. *J. Catal.* **2001**, *197*, 98.
(5) M'Kombe, C. M.; Dry, M. E.; O'Connor, C. T. *Zeolites* **1997**, *19*, 175.
(6) Claude, M. C.; Martens, J. A. *J. Catal.* **2000**, *190*, 39.
(7) van den Broek, A. C. M.; van Grondelle, J.; van Santen, R. A. *J. Catal.* **1997**, *167*, 417.

10.1021/cm0211507 CCC: $22.00
Published on Web 11/07/2002

of NO_x using hydrocarbons in the presence of oxygen.[13−17]

The pretreatment conditions of the support and the noble metal loading method have a strong effect on the metal dispersion in the final catalytic system.[3,5] Several techniques to introduce noble metals into zeolites have been utilized, such as liquid-phase ion exchange, incipient wetness impregnation, vapor impregnation, solid-state ion exchange, and chemical vapor deposition.[7,8,10,12,18] A necessary requirement for the commercial use of the zeolites as supports is to process them into convenient physical forms that can be used in catalytic reactors. The desired macroform is usually achieved by the addition of amorphous binders, which are typically present in amounts of up to 50 wt % of zeolite. The binders, however, dilute the adsorption properties of the zeolite and may slow the rate of mass transfer to and from the zeolite pores. Recently, a method for the preparation of binderless molecular sieve spheres was reported.[19] In this method, zeolite nutrients are ion-exchanged into macroporous anion-exchange resin beads (macrotemplates) and upon hydrothermal treatment the zeolite is crystallized within the pore system of the resin. The combustion of the ion exchanger leads to binderless zeolite spheres with a size and shape similar to those of the original resin beads. Amorphous silica macrostructures have also been prepared by resin macrotemplating.[20] In a recent development of the method, palladium-containing silica spheres were prepared by ion-exchanging $PdCl_4^{2-}$ into resin−silica composite beads employing the ion-exchange capacity retained by the resin after the ion exchange of silica species.[21] The spheres prepared have very high surface areas (up to 1200 $m^2\ g^{-1}$) with the increase of the surface area related to the incorporation of Pd within the silica (the surface area of the pure silica spheres is only 93 $m^2\ g^{-1}$). The present paper reports on the results from the application of the method for the preparation of palladium-containing spheres by resin templating of zeolite materials. Palladium-containing zeolite beta spheres were prepared in which palladium was ion-exchanged into resin-zeolite beta composites employing the residual ion-exchange capacity of the resin.

Experimental Section

Preparation of Palladium-Containing Zeolite Beta Spheres. A macroporous strongly basic Dowex MSA-1 anion-exchange resin (Sigma, chloride ionic form) was used in all experiments as received. The anion exchanger was supplied as spherical particles in the particle size range 20−50 mesh with an ion-exchange capacity of 4 meq g^{-1} specified by the manufacturer. A batch of resin−zeolite beta composites was synthesized by treating the ion exchanger with a clear zeolite beta synthesis solution with molar composition 0.31 Na_2O:9 TEAOH: 0.5 Al_2O_3:25 SiO_2:295 H_2O as described in ref 22. The ionic form of the resin in the resin−zeolite beta composites obtained was assumed to be OH^- as a result of the treatment with the highly alkaline synthesis solution. A part of the resin−zeolite beta composites was charged to an ion-exchange column and the resin was converted into a Cl^- ionic form by passing approximately 10 bed vol of 10 wt % NaCl (Riedel-de Haën, >99.8%). The two resin−zeolite beta composites, in which the resin was in OH^- or Cl^- form, were used to prepare two series of palladium-containing zeolite beta spheres. The amount of solid material obtained from the weight difference between dried (105 °C) resin−zeolite composites and calcined zeolite spheres was ca. 56 wt %. On the basis of this value, calculated amounts of ammonium hexachloropalladate ($(NH_4)_2PdCl_6$, Aldrich, 99%), corresponding to ca. 0.5, 1.0, and 2.0 wt % Pd in the final product, were dissolved in 150 mL of 0.10 M HCl, mixed with 4 g of resin−zeolite beta composites in a beaker and placed on a gyrotary shaker for 24 h. After the ion exchange the initially brownish Pd solutions turned colorless. The composites were separated by decanting, rinsed repeatedly with distilled water, and dried at room temperature. Finally, the organic resin was removed by combustion at 600 °C for 6 h after heating to this temperature at a heating rate of 1 °C min^{-1}. The calcined pure zeolite beta spheres were designated as B(X) were X is OH or Cl, and the palladium-containing ones were designated as B(X)Pd*y* where $y = 0.5$, 1, or 2.

Characterization. The palladium content of the zeolite beta spheres was determined from the difference in concentration of the Pd solutions before and after the ion exchange by flame atomic absorption spectrometry (AAS, Perkin-Elmer 3100). Crystalline phases were identified with a Siemens D5000 powder diffractometer using Cu Kα radiation. UV−vis diffusive reflectance spectroscopy (UV−vis DRS) spectra were obtained with a Perkin-Elmer Lambda 2 UV−vis spectrometer equipped with a Labsphere RSA-PE 20 reflectance spectroscopy accessory and operating in a single-beam mode. A white SRS-99 standard reference material was used for a background correction. Samples were ground into a powder before the X-ray diffraction (XRD) and UV−vis DRS analysis. The morphology of the samples was studied with a Philips XL 30 scanning electron microscope (SEM) equipped with a LaB_6 emission source. A Link ISIS Ge energy-dispersive X-ray detector attached to the SEM was used for evaluation of the palladium distribution over the spheres. The palladium-loaded zeolite spheres were embedded in an epoxy resin (Epofix, Struers) and polished to obtain flat cross sections of the spheres prior to the energy dispersive spectroscopy (EDS) line scan analysis. Nitrogen adsorption measurements were performed with a Micromeritics ASAP 2010 instrument. Samples were outgassed at 300 °C overnight prior to analysis. The total pore volume was obtained by converting the amount adsorbed at a relative pressure of 0.995 to the volume of liquid adsorbate. Pore-size distributions were determined by the BJH method using the desorption branch of the isotherms. The micropore volumes, $V_{\mu p}$, were determined by the *t*-plot method. Chemisorption measurements of the B(Cl)Pd*y* samples were performed with a Micromeritics ASAP 2010C instrument using carbon monoxide as a chemisorbent. The sample was first reduced with H_2 for 2 h at 400 °C followed by evacuation at the same temperature. A CO adsorption isotherm up to 400 mmHg at 35 °C was obtained. The sample was then evacuated at 35 °C for 30 min and the CO isotherm was repeated. The difference between the two straight lines extrapolated to zero pressure was taken as the amount of CO chemisorbed.

(8) Feast, S.; Englisch, M.; Jentys, A.; Lercher, J. A. *Appl. Catal. A* **1998**, *174*, 155.
(9) Blomsma, E.; Martens, J. A.; Jacobs, P. A. *J. Catal.* **1996**, *159*, 323.
(10) Blomsma, E.; Martens, J. A.; Jacobs, P. A. *J. Catal.* **1997**, *165*, 241.
(11) Wang, Z. B.; Kamo, A.; Yoneda, T.; Komatsu, T.; Yashima, T. *Appl. Catal. A* **1997**, *159*, 119.
(12) Lee, J.-K.; Rhee, H.-K. *Catal. Today* **1997**, *38*, 235.
(13) Ogura, M.; Hayyashi, M.; Kage, S.; Matsukata, M.; Kikuchi, E. *Appl. Catal. B* **1999**, *23*, 247.
(14) Ohtsuka, H.; Tabata, T. *Appl. Catal. B* **1999**, *21*, 133.
(15) Shimizu, K.; Okada, F.; Nakamura, Y.; Satsuma, A.; Hattori, T. *J. Catal.* **2000**, *195*, 151.
(16) Park, Y.-K.; Lee, J. W.; Lee, C. W.; Park, S.-E. *J. Mol. Catal. A* **2000**, *158*, 173.
(17) de Correa, C. M.; Cordoba, F.; Bustamante, F. *Microporous Mesoporous Mater.* **2000**, *40*, 149.
(18) Recchia, S.; Dossi, C.; Fusi, A.; Sordelli, L.; Psaro, R. *Appl. Catal. A* **1999**, *182*, 41.
(19) Tosheva, L.; Valtchev, V.; Sterte, J. *Microporous Mesoporous Mater.* **2000**, *35−36*, 621.
(20) Tosheva, L.; Valtchev, V.; Sterte, J. *J. Mater. Chem.* **2000**, *10*, 2330.
(21) Tosheva, L.; Sterte, J. *Chem. Commun.* **2001**, 1112.
(22) Tosheva, L.; Mihailova, B.; Valtchev, V.; Sterte, J. *Microporous Mesoporous Mater.* **2001**, *48*, 31.

Table 1. Pd Loading, Pd Uptake, Micropore ($V_{\mu p}$) and Total Pore (V_p) Volumes of Calcined Macrostructures

sample	palladium loading (wt %)	palladium uptake (%)	micropore volume $V_{\mu p}$ ($cm^3\ g^{-1}$)	total pore volume V_p ($cm^3\ g^{-1}$)
B(OH)	–	–	0.18	0.64
B(OH)Pd0.5	0.49	100.0	0.12	0.81
B(OH)Pd1	1.04	99.4	0.10	0.80
B(OH)Pd2	2.01	99.3	0.09	0.68
B(Cl)	–	–	0.10	0.72
B(Cl)Pd0.5	0.50	100.0	0.12	0.82
B(Cl)Pd1	1.06	99.6	0.11	0.77
B(Cl)Pd2	2.29	99.5	0.11	0.71

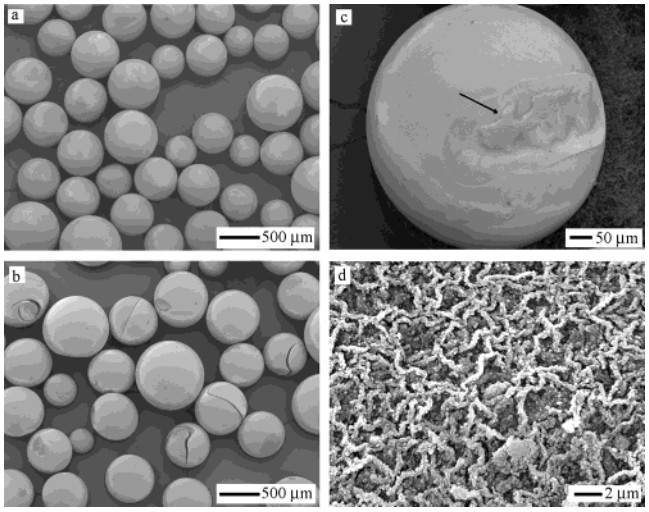

Figure 1. SEM images of zeolite beta spheres (a), palladium-containing zeolite beta spheres (b), and a Pd sphere at higher magnifications (c, d).

Palladium dispersions were calculated on Pd/CO = 1:1 basis. Three consecutive measurements were performed on each sample.

Results and Discussion

General Characterization. The measured palladium contents of the zeolite beta spheres are listed in Table 1. The palladium uptake is also given in this table in order to demonstrate the completion of the ion exchange reaction. A lower micro- and a higher total pore volume was obtained for the pure beta B(Cl) sample compared to the pure beta B(OH) sample. This could be due to the reversion of the resin into a Cl^- form. The values of the micropore volume of the palladium-containing samples were generally similar independent of the ionic form of the resin, Cl^- or OH^-, and of the palladium loading *y*. On the other hand, a slight increase in the total pore volumes was obtained for the Pd samples compared to the pure beta ones, which may be attributed mainly to changes in the mesopore volumes. These results differ from the results for Pd silica spheres, where a substantial increase in the pore volumes due to the palladium insertion was observed.[21]

Visually, the palladium-containing spheres obtained after the calcination were brownish, with the color intensity increasing with an increase in the Pd loading. A SEM image of the initial zeolite beta spheres is shown in Figure 1a. Those spheres were similar in size and shape to the original resin beads. The spheres were built up by fine crystals with a size of about 100 nm, which is similar to the pore size of macroporous ion-exchange resins (not shown).[22] Larger crystals with a size of up to 400 nm were observed on the sphere surfaces, where there were no steric limitations for the crystal growth due to the presence of the resin polymer chains (not shown). Nevertheless, the surfaces were very homogeneous. The palladium-containing spheres were similar in shape and size to the original resin beads as well (Figure 1b). However, the particles were of inferior mechanical stability and a certain number of cracked spheres were observed. The number of cracked and broken particles increased with increasing the Pd loading. Again, such a deterioration of the mechanical stability related to the Pd insertion was not previously observed for the Pd silica spheres prepared by resin macrotemplating.[21] Further, regions of differing appearance were observed on the surfaces of the Pd-containing spheres (Figure 1b,c). The crystals in these areas were arranged as shown in Figure 1d. No other differences were observed in the SEM micrographs between the palladium-containing spheres and the pure beta ones.

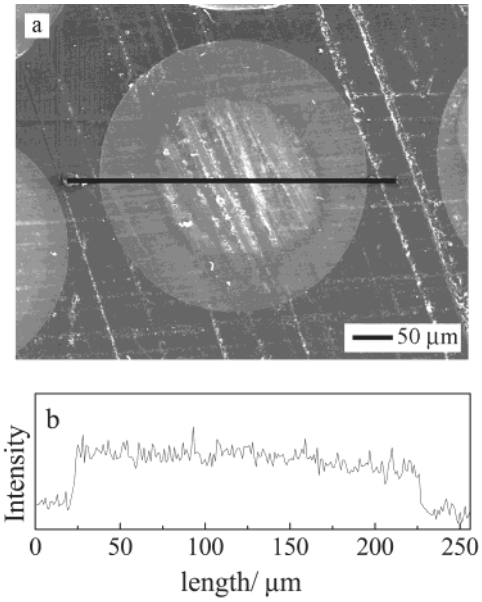

Figure 2. SEM image of a cross-sectioned Pd-beta sphere (a) and EDS line scan analysis of palladium over it (b).

Table 2. Values for Pd Dispersion and Pd Surface Area for Calcined B(Cl)Pd*y* Spheres Obtained from Three Consecutive Chemisorption Measurements for Each Sample

	Pd dispersion/%			Pd surface area $m^2\ g^{-1}$ metal		
sample	1	2	3	1	2	3
B(Cl)Pd0.5	32.3	15.9	15.1	144.1	70.9	67.3
B(Cl)Pd1	9.5	5.9	5.8	42.2	26.2	25.7
B(Cl)Pd2	8.4	7.2	6.0	37.6	32.2	26.7

The palladium distribution over the spheres prepared was studied by EDS line scan analysis. Figure 2 shows a SEM image of a cross-sectioned palladium-containing zeolite beta sphere (a) and the corresponding Pd line scan over it (b). As shown, the palladium was homogeneously dispersed within the sphere. Similar results were obtained for all the palladium-containing samples.

The Pd dispersions and Pd surface areas of the B(Cl)-Pd*y* samples are given in Table 2. The dispersions were in the range 8.4−32.3% and decreased with an increase in the Pd loading, probably due to agglomeration. In repeated measurements, even lower dispersions were measured, perhaps due to sintering. The effect was most

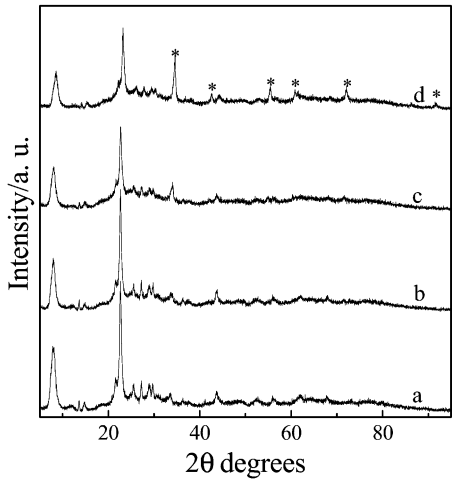

Figure 3. XRD patterns of calcined B(OH) (a), B(OH)Pd0.5 (b), B(OH)Pd1 (c), and B(OH)Pd2 (d) spheres. Peaks with asterisks correspond to PdO.

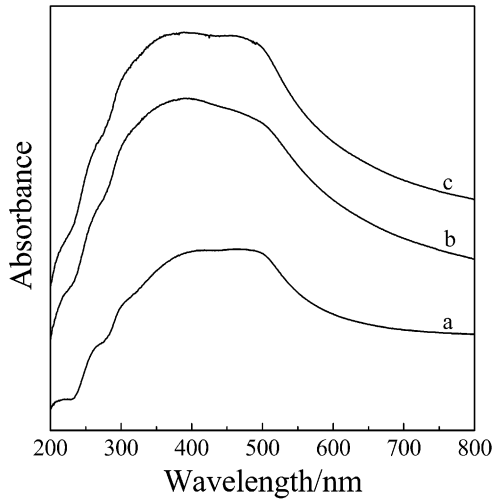

Figure 4. UV-vis DRS spectra of B(Cl)Pd0.5 (a), B(Cl)Pd1 (b), and B(Cl)Pd2 (c) samples.

pronounced in the B(Cl)Pd0.5 sample, for which the dispersion value from the second measurement was half that of the first measurement. No substantial differences were observed between the second and the third measurements.

XRD was used to further characterize the palladium-containing spheres. XRD patterns of the B(OH) and B(OH)Pd*y* samples are shown in Figure 3. All the palladium beta spheres were highly crystalline, though a certain decrease in the intensity of the zeolite beta reflection peaks, proportional to the Pd content, was observed. Additional peaks corresponding to PdO were detected in the samples containing 1.0 and 2.0 wt % palladium. Similar results were obtained for the B(Cl)-Pd*y* samples.

Figure 4 shows the UV−vis DRS spectra of the palladium-containing zeolite beta spheres obtained from the composites in the Cl^- ionic form. A broad complex band in the range 300−500 nm was observed for all samples indicating the presence of PdO species.[16] In addition, the brownish color of the spheres is believed to be due to the presence of Pd^{2+} species bound to the oxygen of the support.[23,24] Similar spectra were obtained for the palladium-containing samples obtained from the composites in the OH^- form.

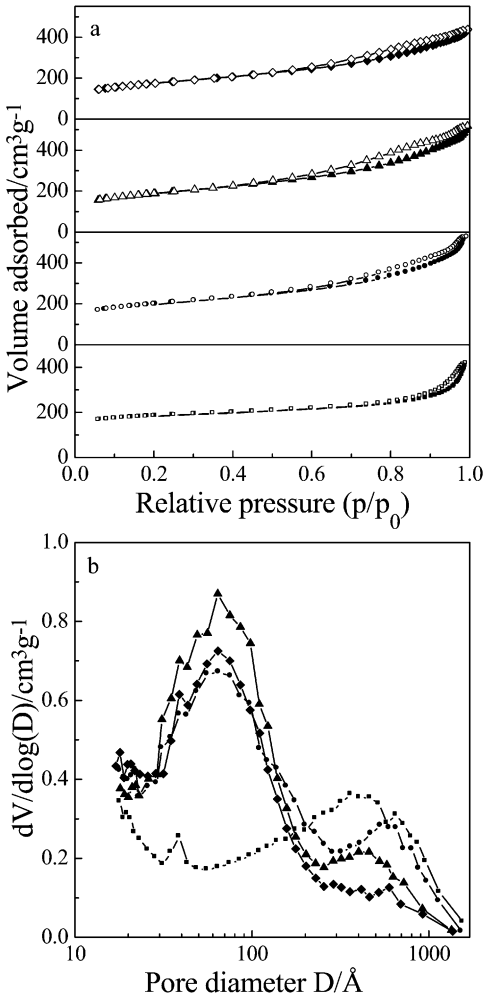

Figure 5. Nitrogen adsorption isotherms for calcined B(OH) and B(OH)Pd*y* samples: solid symbols adsorption, open symbols desorption (a). Corresponding BJH desorption pore volume plots (b): ■, B(OH); ●, B(OH)Pd0.5; ▲, B(OH)Pd1; ◆, B(OH)-Pd2.

Pore Structure. The nitrogen adsorption isotherms and the corresponding BJH pore-size distributions for the B(OH) and B(OH)Pd*y* samples are shown in Figure 5. The isotherms were all of type IV typical of mesoporous materials but micropores due to the zeolite were also present. The mesoporosity was created by the removal of the organic ion exchanger.[19] The hysteresis loop recorded in the isotherm of the pure zeolite beta sample may be determined as type H1, which is obtained for agglomerates of spheroidal particles of fairly uniform size and array.[25] The shape of the hysteresis loop in the isotherms of the palladium-containing samples was different, probably due to a change in the shape of the pores as a result of the Pd insertion. Also, the isotherms for the B(OH)Pd*y* spheres were very similar to each other. A substantial part of the pore volume of the B(OH) spheres was found in the mesopores with a size of ca. 400 Å (Figure 5b). The distribution was changed for the palladium-containing spheres. Two peaks can be distinguished in the BJH

(23) Kovala-Demertzi, D.; Tsangaris, J. M.; Hadjiliadis, N. *Transition Met. Chem.* **1984**, *9*, 77.
(24) Attyia, K. M. E.; Fouad, N. E. *J. Thermal Anal.* **1994**, *42*, 1207.
(25) Gregg, S. J.; Sing, K. S. W. *Adsorption, Surface Area and Porosity*; Academic Press: London, 1982.

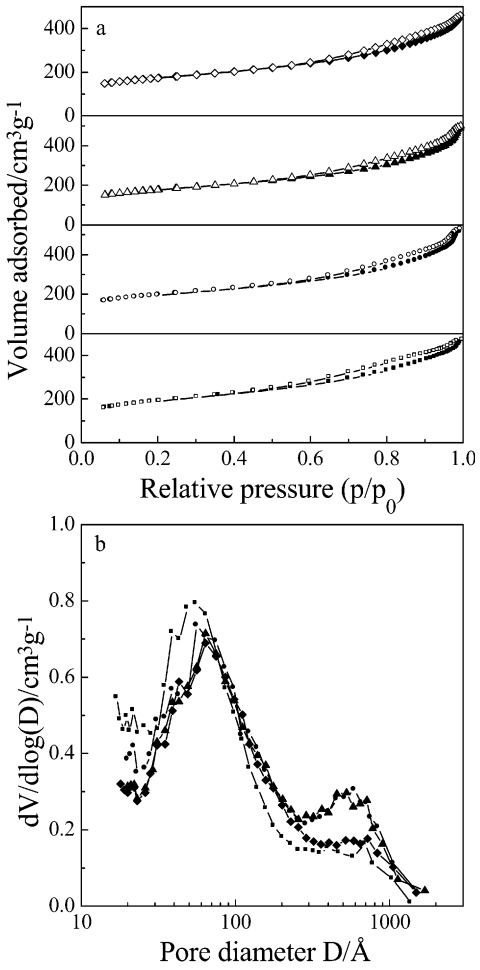

Figure 6. Nitrogen adsorption isotherms for calcined B(Cl) and B(Cl)Pd*y* samples, solid symbols adsorption, open symbols desorption (a). Corresponding BJH desorption pore volume plots (b): ■, B(Cl); ●, B(Cl)Pd0.5; ▲, B(Cl)Pd1; ◆, B(Cl)Pd2.

pore-size distribution curves: an intense one centered at ca. 70 Å which is similar for the samples of varying Pd contents, and a broader one of a lower intensity above 200 Å. The latter peak decreased with an increase in the palladium loading. Similar trends were observed for the isotherms and the pore-size distributions of the B(Cl)Pd*y* samples (Figure 6). A difference was, however, obtained in the isotherm and the BJH pore-size distribution of the B(Cl) sample compared to that of B(OH). The change is most likely related to a change in the organic polymer network as a result of the reversion of the resin into a Cl^- form. The result may be used to prepare zeolite spheres with tailored mesoporosity by the resin templating method. Comparing Figures 5 and 6 it can be concluded that the ionic form of the resin−zeolite beta composites has little influence on the pore structure of the palladium-containing zeolite beta spheres.

Conclusions

Palladium-containing zeolite beta spheres were prepared by a multistep procedure using macroporous anion-exchange resin as a macrotemplate. Palladium anion species were introduced by ion exchange into resin−zeolite beta composites obtained after the hydrothermal treatment of a mixture of resin beads and zeolite beta synthesis solution. Upon removal of the resin by calcination self-bonded palladium containing zeolite beta spheres remain. Samples of controllable Pd content were prepared by the method. The mechanical stability of the spheres deteriorated with an increase in the Pd loading. Palladium was homogeneously distributed within the spheres but relatively poorly dispersed. The Pd dispersions decreased with an increase in the Pd content. Palladium in the zeolite spheres was present in the form of PdO. The pore structure of the samples prepared consisted of both micropores (from the zeolite) and meso/macropores (from the resin removal). A comparison with previously reported results for Pd silica spheres shows that the mechanical stability and the pore structure of the Pd-containing spheres prepared by resin macrotemplating is very sensitive to the type of the inorganic support: amorphous silica or zeolite.

A major advantage of the method presented is that the macrostructures prepared may be directly used as catalysts (e.g., in fixed-bed reactors) thus excluding further processing to form macroparticles and avoiding deterioration effects due to the addition of binders in conventionally prepared zeolite-supported catalysts. This makes the palladium-containing zeolite beta spheres prepared according to the method potentially beneficial catalysts in, for instance, the field of organic syntheses, where current trends in catalysts design are toward reducing the number of individual reactions taking place during the conversion, for example, by using multifunctional catalytic systems.

Acknowledgment. The partial financial support from the Swedish Research Council for Engineering Sciences (VR) is gratefully acknowledged.

CM0211507